EPJ manuscript No.
(will be inserted by the editor)

Hadron Multiplicity in Semi-Inclusive Lepton-Nucleon and Lepton-Nucleus Scattering

O. Benhar[1], S. Fantoni[2], G.I. Lykasov[3], U. Sukhatme[4], and V.V. Uzhinsky[3]

[1] INFN and Physics Department, Università "La Sapienza". I-00185 Roma, Italy
[2] International School for Advanced Studies (SISSA). I-34014 Trieste, Italy
[3] Joint Institute for Nuclear Research. Dubna, Moscow Region, 141980 Russia
[4] State University of New York at Buffalo. Buffalo, NY 14260-4600, USA

arXiv:nucl-th/0310003v1 1 Oct 2003

Received: date / Revised version: date

Abstract. We discuss multi-hadron production in both inelastic neutrino-nucleon interactions in the current fragmentation region and neutrino-nucleus collisions in the target fragmentation region. Our analysis, carried out within the framework of the quark-gluon string model, is mainly focused on the difference between these two processes. We show that the Q^2 dependence of hadron multiplicity in the current and target fragmentation regions is indeed completely different. The study of inelastic $\nu - A$ scattering in the target fragmentation region also provides new information on nuclear structure at small $N - N$ distances. The results of the proposed approach are in satisfactory agreement with the data recently obtained at CERN by the NOMAD Collaboration.

PACS. 13.60.Hb Total and inclusive cross sections – 13.15.+g Neutrino interactions

1. Introduction

Deep-inelastic particle interactions play a decisive role in the development of the modern theory of fundamental interactions. For instance, the investigation of multi-hadron production in inelastic scattering of leptons off nucleons and nuclei is a tool to study both the dynamics of such processes and the quark structure of the target. Of particular interest, in this context, is the analysis of the Q^2 dependence over a wide range of values. The difficulties associated with the increase of the QCD coupling constant $\alpha_s(Q^2)$ at moderate and low Q^2 have led to the development of alternative approaches to analyze soft hadron interactions. A well known example is the the $1/N$ expansion of the scattering amplitude, N being the number of colors or quark flavors, suggested by t'Hooft [1] and Veneziano [2]. Based on this approach, the Quark-Gluon String Model (QGSM) and the Dual Parton Model (DPM) have been developed in Refs.[3] and [4,5], respectively, to analyze hadronic reactions. The first application of the QGSM to inelastic lepton-nucleon processes at moderate and low Q^2 has been carried out in Ref.[6].

In this paper we investigate inelastic neutrino scattering from both protons and nuclei within the QGSM, focusing mainly on the differences between these reactions. In Section 2 we outline the main features of the theoretical approach, whereas Section 3 is devoted to a comparison between our results and the data recently obtained at CERN by the NOMAD collaboration. Finally, in Section 4 we summarize our findings and state the conclusions.

2. Theoretical framework

In the QGSM [3,6], hadron production in the reactions $\nu(\bar{\nu}) + p \to \mu^-(\mu^+) + h + X$ is described in terms of planar and cylindrical graphs, as shown in Fig.1. The planar graph of panel (a) describes neutrino scattering off a valence quark, corresponding to one Reggeon exchange in the t-channel [6], whereas the cylindrical graph of panel (b) describes neutrino scattering off sea quarks, corresponding to one-Pomeron exchange in the t-channel [6]. The figure also shows the occurrence of hadronization in the colorless quark-antiquark and quark-diquark strings.

The relativistic invariant distribution of hadrons produced in the process $\nu(\bar{\nu}) + p \to \mu^-(\mu^+) + h + X$ is defined as

$$\rho_{\nu(\bar{\nu})+p\to\mu^-(\mu^+)+h+X} \;=\; E_h \frac{dN}{d^3p_h d\Omega dE'} \;, \qquad (1)$$

where E_h and $\mathbf{p}_h$ are the total energy and three momentum of the produced hadron, respectively, whereas E' and Ω are the energy and the solid angle of the final state muon. The right hand side of Eq.(1) can be written in the following general form [7,8]:

$$\rho_{\nu(\bar{\nu})+p\to\mu^-(\mu^+)+h+X} = \Phi(Q^2)\left\{F_P(x,Q^2;z,p_{ht}) + F_C(x,Q^2;z,p_{ht})\right\} \;, \qquad (2)$$

with

$$\Phi(Q^2) \;=\; mE\frac{G^2}{\pi}\frac{m_W^2}{Q^2+m_W^2} \;, \qquad (3)$$

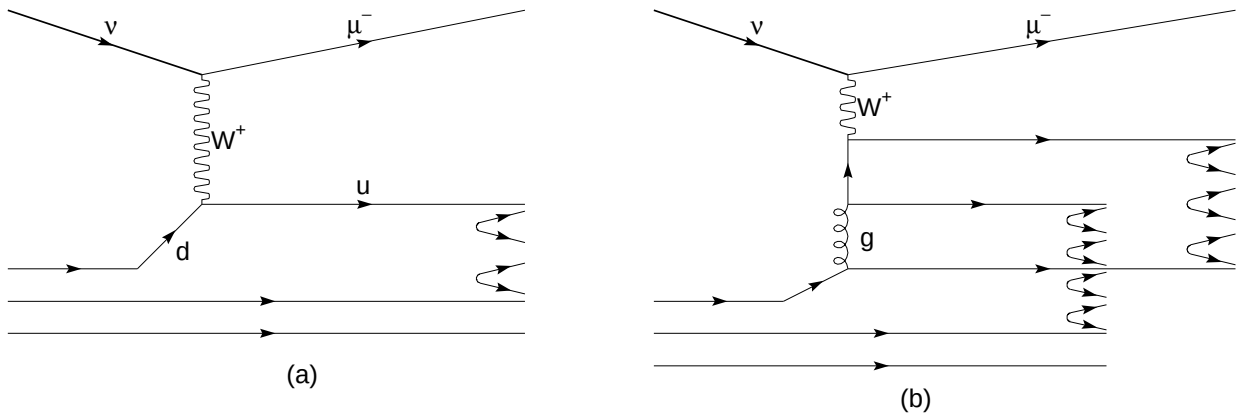

Fig. 1. Planar, one-Reggeon exchange (panel (a)), and cylindrical, one-Pomeron exchange (panel (b)), graphs (see text).

where G is the Fermi weak coupling constant, E is the energy of the incoming neutrino, m and m_W are the nucleon and W-boson masses, respectively, $x = Q^2/2(p_\nu \cdot k)$ is the Bjorken variable and p_ν and k are the four momenta of the initial neutrino and nucleon. In general, z is the light cone variable defined as $z = (E_h + p_{hz})/(E + p_z)$, where p_{hz} is the component of the hadron momentum parallel to the momentum of the incoming neutrino, p_z, (see, e.g., Refs.[3,6] and [4,5]). At large energies of the final hadron it reduces to the longitudinal momentum fraction of the hadron, with respect to the neutrino, in the rest frame of the target proton. The variable z can also be treated as the Feynman variable $x_F = 2p_L^*/W_X$, defined as the longitudinal momentum fraction in the hadronic center of mass system (HCMS). Here p_L^* denotes the longitudinal hadron momentum in the HCMS and W_X is the mass of the hadrons produced in the reaction. Finally, p_{ht} is the transverse momentum of the produced hadron with respect to the current (hadronic jet) direction, (see, e.g. Ref.[9]).

The probabilty distributions of hadron production associated with the planar and cylindrical graphs of Fig.1 are given by $F_P(x, Q^2; z, p_{ht})$ and $F_C(x, Q^2; z, p_{ht})$, respectively. They can be computed either analytically, as in Ref.[7], or using the Monte Carlo (MC) approach to generate all quark-antiquark and quark-diquark strings shown in Fig.1, as done in Ref.[8].

The main ingredients for the calculations of observables in the reaction under discussion are the quark distributions in a nucleon and their fragmentation functions to hadrons. In addition to the dependence upon x, quark distributions also depend on Q^2 and the transverse momentum k_t. Following Ref. [7], we use a factorized form for these distributions:

$$q_f(x, Q^2; k_t) \;=\; q_f(x, Q^2) g_q(k_t) \;, \qquad (4)$$

with the function g_q chosen in the form

$$g_q(k_t) \;=\; \frac{B^2}{2\pi} e^{-Bk_t} \;, \qquad (5)$$

where $B = 1/\langle k_t \rangle \simeq 4(GeV/c)^{-1}$, while $\langle k_t \rangle \simeq 0.25$ GeV/c is the average transverse momentum of a quark in a nucleon. As for the function $q_f(x, Q^2)$, we use the fit suggested in Ref.[10], including true Regge x-asymptotic at $x \to 0, x \to 1$ and small Q^2, and its QCD prediction at large Q^2.

In general, the fragmentation functions (FF) of quarks (diquarks) into hadrons, $D^h_{q(qq)}$, depend on the hadron momentum fraction z_1 and the hadron transverse momentum with respect to a quark (diquark) momentum direction, $\widetilde{p}_{ht}$. Here we choose again the factorized form

$$D^h_{q(qq)}(z_1, \widetilde{p}_{ht}) \;=\; D^h_{q(qq)}(z_1) g_q(\widetilde{p}_{ht}) \;, \qquad (6)$$

with the function g_q defined as in Eq.(5).

The functions $D^h_{q(qq)}(z_1)$ are obtained, according to the recursive cascade model procedure suggested in [11], from the integral equation

$$D^h_{q(qq)}(z_1) \;=\; f(z_1) \;+\; \int_{z_1}^1 \frac{dx}{x} f(x) D^h_{q(qq)}\left(\frac{z_1}{x}\right) \;, \qquad (7)$$

the function $f(x)$ being chosen in the form

$$f(x) \;=\; x^\beta (1-x)^\gamma \;. \qquad (8)$$

According to the main assumptions underlying the QGSM, the fragmentation functions $D^h_{q(qq)}(z_1)$ should satisfy true Regge asymptotic at $z_1 \to 1$ and $z_1 \to 0$ [3]. These constraints determine the values of the parameters. The detailed procedure is presented in Ref.[12]. In general the FF depend not only on z_1 and p_{ht}, but also on Q^2. At low Q^2 they have to reproduce the true Regge asymptotic [3], while at large Q^2 they have to describe e^+e^- annihilation data. As we mainly analyze inelastic $\nu - N$ interactions at moderate Q^2, one can assume that the Q^2-dependence of the FF be negligibly weak.

Let us now consider pion production in the target fragmentation region in $\nu - A$ interactions. Our study of these processes focuses on the kinematical region of large pion

momentum ($p_\pi > 0.3$ GeV/c), where the effects of final state interactions (FSI), leading to pion absorption associated with production of baryon resonances, are expected to be small [13,14] and the impulse approximation (IA) cane be safely used.

Within the framework of the IA the relativistic invariant semi-inclusive spectrum of hadrons, in particular pions, produced by the semi-inclusive inelastic process $\ell + A \to \ell' + \pi + X$,

$$\rho_{\ell+A\to\ell'+\pi+X} \equiv E_h d\frac{\sigma}{d^3p_h d\Omega dE'} \ , \tag{9}$$

can be written in the convolution form [7]

$$\rho_{\ell+A\to\ell'+\pi+X}(x,Q^2;z,p_t) = \int_{z\le y} dy d^2k_t f_A(y,Q^2,k_t) \times \left[\frac{Z}{A}\rho_{\ell+p\to\ell'+\pi+X}(x/y,Q^2;z/y,p_t-k_t) + \frac{N}{A}\rho_{\ell+n\to\ell'+\pi+X}(x/y,Q^2;z/y,p_t-k_t)\right] \ , \tag{10}$$

where Z, N and A are the numbers of nucleons, protons and neutrons in the nucleus, $z = (pp_\nu)/(P_A p_\nu)M_A/m$, p is the four-momentum of the produced pion and M_A and m are the nucleus and nucleon masses, respectively. $\rho_{\ell+p(n)\to\ell'+\pi+X}$ denotes the semi-inclusive spectra of pions produced by interactions of the lepton ℓ with a quasi-free proton (neutron). The nucleon distribution function $f_A(y,k_t)$ is defined as [15]

$$f_A(y,k_t) = \int dk_0 dk_z S(k) y\delta\left(y - \frac{M_A}{m}\frac{(kq)}{(P_A q)}\right) \ , \tag{11}$$

where q is the four-momentum transferred by the lepton, $q^2 = -Q^2$, $S(k)$ is the relativistic invariant function describing the nuclear vertex with an outgoing virtual nucleon, $y = (M_A/m)(kp_\nu)/(P_A p_\nu)$ and P_A ,k and p_ν are the four-momenta of the nucleus, nucleon and initial neutrino, respectively.

The distribution function $f_A(y)$, defined as the integral of $f_A(y,k_t)$ over d^2k_t, can be calculated within nuclear many-body theory approximating $S(k)$ with the nonrelativistic spectral function $P(k,E)$, yielding the probability of finding a nucleon with momentum $\mathbf{k}$ and removal energy $E = m - k_0$ [16]. However, due to the limited range of momentum and removal energy covered by nonrelativistic calculations of $P(k,E)$ (typically $|\mathbf{k}| < k_{min} \sim 0.7 - 0.8$ GeV/c and $(m - k_0) < 0.6$ GeV, see e.g. [16]), this procedure can only be used in the region $y < y_0 \sim 1.7 - 1.85$. An alternative approach to obtain $f_A(y)$ at larger y, based on the calculation of the overlap of the relativistic invariant phase-space available to quarks belonging to strongly correlated nucleons, has been proposed in Refs.[15,17].

The convolution form of Eq.(11) implies that to analyze the production of pions emitted in the whole backward hemisphere by $\nu - A$ interaction one needs to know the dependence of the nucleon distribution upon y and k_t. We assume the following factorized form:

$$f_A(y,k_t) = f_A(y) g_A(k_t) \ , \tag{12}$$

where the function g_A is chosen to be a Gaussion

$$g_A(k_t) = \frac{1}{\pi\langle k_t^2\rangle}\exp(-k_t^2/\langle k_t^2\rangle) \ , \tag{13}$$

$\langle k_t^2\rangle$ being the average value of the squared transverse momentum of a nucleon in the target nucleus.

3. Comparison to data

The results of our calculation of different observables of the reactions $\nu + N \to \mu^- + h + X$ and $\nu + C^{12} \to \mu^- + \pi^- + X$ are presented in Figs.2−4.

The mean charged multiplicity in the current region is shown in Fig.2. The multiplicity measured by the NOMAD collaboration [18], $\langle n_{ch}\rangle$, turns out to be close to $\langle n_{ch}\rangle/2$ measured in e^+e^- experiment at energy $E = \sqrt{s}$ and to $\langle n_{ch}\rangle$ obtained from ep and $\bar\nu_\mu p$ at $E = Q$. In Fig.2 we compare our results to $\langle n_{ch}^{QCD}\rangle/2$ obtained from a QCD calculation of the charged multiplicity in e^+e^-. The QCD results, represented by open circles, correspond to evolution of parton distributions in the leading log approximation, yielding the following fit for $\langle n_{ch}^{QCD}\rangle$ (see Ref.[18]):

$$n_{ch}^{QCD} \ = \ a + b\,\exp\left(c\sqrt{\log(Q^2/Q_0^2)}\right) \ , \tag{14}$$

where $a = 2.257$, $b = 0.094$, $c = 1.775$ and $Q_0 = 1$ GeV/c. The solid, long-dash and short-dash lines in Fig.2 correspond to our Monte Carlo calculations at initial neutrino energies $E_\nu = 150$ GeV, $E_\nu = 45$ GeV, $E_\nu = 23.6$ GeV, respectively. The NOMAD experimental data are averaged over the initial energy [18].

Fig.2 shows that the QCD fit, while failing to reproduce the NOMAD data on the charged multiplicity at $Q < 5$ GeV/c, provides a reasonable description of the behavior at large Q. As discussed in [18] the same fit also satisfactorily describes $\langle n_{ch}\rangle$ obtained from e^+e^-, ep and $\bar\nu_\mu p$ experiments. On the other hand, the approach proposed in Ref.[8] describes the NOMAD data at $Q < 5$ GeV/c rather well.

The multiplicity of pions, normalized to the cross section of the process $\nu + A \to \mu + X$, σ, is defined as

$$\langle\widetilde{n}_\pi\rangle \equiv \frac{\langle n_\pi\rangle}{\sigma} = \frac{1}{\sigma}\int_{x_{min}}^{x_{max}} dx \times \int_{z_{min}}^{z_{max}}\frac{dz}{z}\int_0^{p_{max}} d^2p\ \rho_{\nu+A\to\mu+\pi+X} \ . \tag{15}$$

It can be split in two parts, corresponding to the planar,or one-Reggeon exchange, diagram (Fig.1 (a)) and cylindrical, or one-Pomeron exchange graph (Fig.1 (b)).

The NOMAD collaboration carried out a study of inelastic $\nu - C$ interactions in which the negative pions emitted in the whole backward hemisphere, with respect to the incoming neutrino beam, were detected [9]. The data of Fig.3 show the nultiplicity of negative pions carrying momenta $0.35 < p_\pi < 0.8$ GeV/c, measured in a kinematical

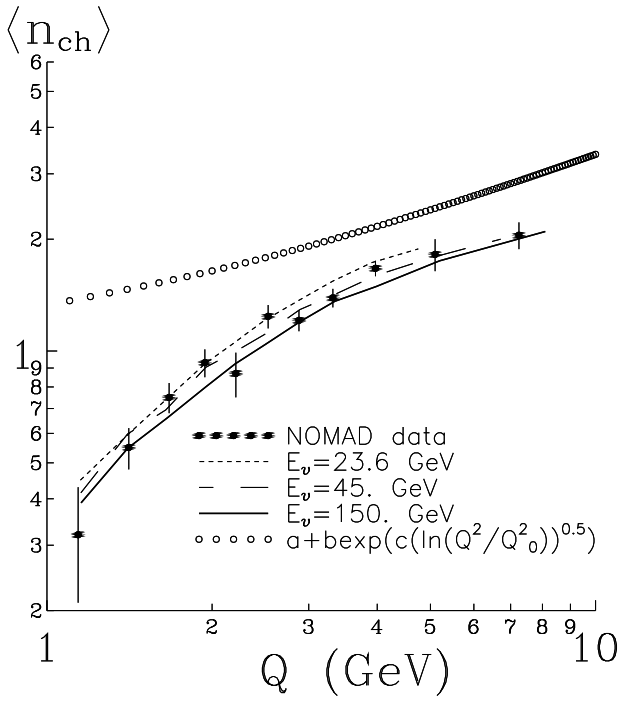

Fig. 2. Mean multiplicity of charged hadrons in the current fragmentation region for the process $\nu + p \rightarrow \mu^- + h + X$, as a function of the momentum transfer Q. The open circles correspond to the QCD fit given by eq.(14), while the solid, long-dash and short-dash lines correspond to our calculations at $E_\nu = 150$, 45 and 23.6 GeV, respectively. The experimental data are taken from Ref.[18]

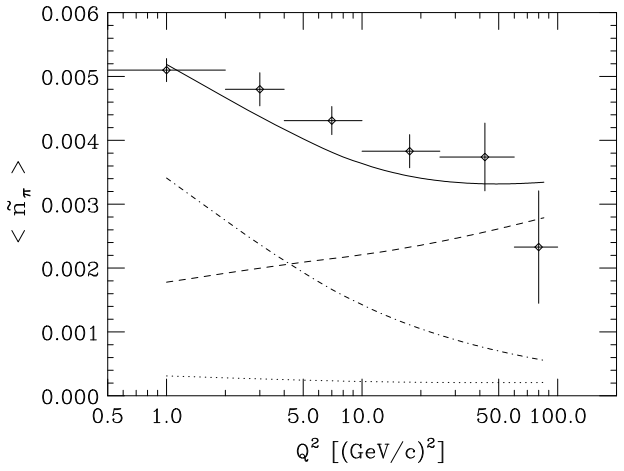

Fig. 3. Mean multiplicity of charged pions produced in the backward hemisphere in $\nu - C$ interaction as a function of Q^2. The solid line shows the results of the full calculation, including both graphs of Fig.1. The dashed and dash-dot lines correspond to the separated contributions of the cylindrical graph of Fig.1 (b) and the planar graph of Fig.1 (a), respectively. The dots show the results obtained setting $P(\mathbf{k}, E) \equiv 0$ in the high energy-momentum domain, not covered by the nonrelativistic calculation of Ref.[16]. The experimental data are taken from Ref.[9].

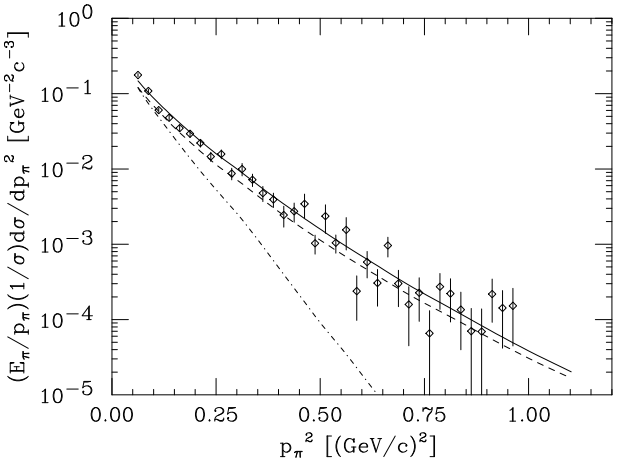

Fig. 4. p_π^2 -dependence of the spectrum of backward pions produced in inelastic $\nu - C$ interaction. The solid curve corresponds to the full calculation whereas the dashed line has been obtained including only the cylindrical graph of Fig.1 (b). The dash-dot line shows the results obtained setting $P(\mathbf{k}, E) \equiv 0$ in the high energy-momentum domain, not covered by the nonrelativistic calculation of Ref.[16]. The experimental data are taken from Ref.[9].

setup in which W_X increases as Q^2 increases. Theoretical calculations have been performed applying the same kinematical conditions.

As shown in Fig.3, the planar graph provides the main contribution at small Q^2, while the cylindrical one dominates at $Q^2 > 10$ (GeV/c)^2. It clearly appears that both diagrams have to be included to explain the observed Q^2 dependence. The dotted line in Fig.3 has been obtained setting $P(\mathbf{k}, E) = 0$ in the domain of large energy and large momentum, not covered by the nonrelativistic calculations of ref.[16]. Comparison between the solid and dotted line shows that the dominant contribution to $< \widetilde{n}_\pi >$ does indeed come from the high momentum tail of the nucleon distribution.

In Fig.4 we compare the p_π^2 dependence of the experimental spectrum to the one resulting from our approach. The contribution of the cylindrical graph dominates the spectrum and the inclusion of the high momentum tail of the nucleon distribution, corresponding to $p > 0.4$ GeV/c, is clearly needed to describe the data.

4. Summary and conclusions

In this paper we have analyzed inelastic $\nu - N$ and $\nu - A$ processes at low and moderate Q^2 within the QGSM. The main conclusions can be summarized as follows. The dynamics of hadron production in the current fragmentation and target fragmentation regions is different. At low Q^2 the contribution of the cylindrical graph to the hadron multiplicity is much more prominent in the first kinematical region than it is in the second one. There is some analogy between pion production in the backward hemisphere from target fragmentation and soft $h - N$ processes at

$x_F \to -1$, where the one-Pomeron exchange graph dominates at large initial energy (see, e.g., Ref.[6]). In conclusion, the contributions of the graphs of Figs.1 (a) and (b) have different Q^2 dependences in the different kinematical regions corresponding to current and target fragmentation.

The conventional perturbative QCD calculations of hadron multiplicities, both in $\nu - N$ and $\nu - A$ inelastic interactions, do not reproduce the NOMAD data, whereas the application of the QGSM allows for a rather satisfactory description. As for the role of nuclear structure, the dominant contribution to the spectrum of pions emitted in the backward hemisphere in $\nu - A$ inelastic scattering is clearly coming from the high momentum tail of the nucleon distribution, which can be described in terms of overlaps of distributions of three-quark colorless objects [19].

References

1. G. t'Hooft, Nucl.Phys. **B72**, (1974) 461.
2. G. Veneziano, Phys.Lett. **B52**, (1974) 200.
3. A.B. Kaidalov, Phys. Lett. **B116**, (1982) 459 ; Sov. J. Nucl. Phys. **45**, (1987) 902.
4. A. Capella, U. Sukhatme, C.I. Tan and J. Tran Thanh Van, Phys. Lett. **B81**, (1979) 68 : Z. Phys. **63**, (1979) 68.
5. A. Capella, U. Sukhatme, C.I. Tan and J. Tran Thanh Van, Phys. Rep. **236**, (1994) 223.
6. A.B. Kaidalov, Sov. J. Nucl. Phys. **33**, (1981) 733.
7. O. Benhar, S. Fantoni, G.I. Lykasov and U. Sukhatme, Phys. Lett. **B527**, (2002) 73.
8. G.I. Lykasov, U. Sukhatme and V.V. Uzhinsky, Phys. Lett. **B553**, (2003) 217.
9. NOMAD Collaboration, P. Altegoer *et al*, Phys. Lett. **B455**, (1999) 439.
10. A. Capella, A. Kaidalov, C. Merino and J. Tran Thanh Van, Phys. Lett. **B337**, (1994) 358 ; Phys. Lett. **B343**, (1995) 403 ; A. Kaidalov and C. Merino, Eur. Phys. J. C **10**, (1999) 153.
11. R.D. Field and R. P. Feynman, Nucl. Phys. **B136** (1978) 1; U. Sukhatme, Phys. Lett. **B73**, (1978) 478 ; Zeit. Phys. **C2**, (1979) 321; U. Sukhatme, K. Lassila and R. Orava, Phys. Rev. **D25**, (1982) 2975.
12. V.V. Uzhinsky and S.Yu. Shmakov, Sov. J. Nucl. Phys. **53**, (1991) 1034.
13. L.L. Frankfurt and M.I. Strikman, Phys. Rep. **160**, (1988) 236.
14. N.S. Amelin and G.I. Lykasov, Sov. J. Nucl. Phys. **33**, (1981) 100.
15. O. Benhar, S. Fantoni, G.I. Lykasov and N.V. Slavin, Phys.Rev. C **57**, (1998) 1532.
16. O. Benhar, A. Fabrocini and S. Fantoni, Nucl. Phys. **A505**, (1989) 267.
17. O. Benhar, S. Fantoni and G.I. Lykasov, Eur. Phys. J. A **7**, (2000) 415.
18. NOMAD Collaboration, J. Altegoer, *et al*, Phys. Lett. **B445**, (1999) 439.
19. O. Benhar, S. Fantoni, G.I. Lykasov and N.V. Slavin, Phys. Rev. C **55**, (1997) 244.